AIAA JOURNAL
Vol. 30, No. 12, December 1992

Streamwise Evolution of a Square Jet Cross Section

W. R. Quinn*
St. Francis Xavier University, Antigonish, Nova Scotia, B2G 1C0 Canada

Results of an experimental study of a turbulent free jet of air issuing from a sharp-edged square slot into still air surroundings are presented. The study was done to shed some light on the streamwise development of the jet cross section. The quantities measured directly, using hot-wire anemometry, include the three components of the mean velocity vector, the three Reynolds normal stresses, and the two Reynolds primary shear stresses. It was found that the near region of the jet is dominated by four sets of counter-rotating streamwise vortices. These vortices, which represent Prandtl's secondary flow of the first kind, are generated from distributed vorticity shed from the four corners of the slot by skewing of the shear layers as a result of the vena contracta effect. Mean streamwise velocity off-center peaks were also found in the very near region; such mean streamwise velocity off-center peaks may be the result of the self-induction of the streamwise vortices. Furthermore, the higher numerical values of the Reynolds normal and primary shear stresses in the present square jet, compared with those found in a round jet, indicate faster mixing of the square jet.

Nomenclature

D = diameter of a round slot
D_e = equivalent diameter
$\overline{U}$ = mean streamwise velocity
$\overline{u'^2}$ = streamwise Reynolds normal stress
$\overline{u'v'}$ = spanwise Reynolds primary shear stress
$\overline{u'w'}$ = lateral Reynolds primary shear stress
$\overline{V}$ = mean spanwise velocity
$\overline{v'^2}$ = spanwise Reynolds normal stress
$\overline{W}$ = mean lateral velocity
$\overline{w'^2}$ = lateral Reynolds normal stress
X = streamwise coordinate
Y = spanwise coordinate
Z = lateral coordinate
Ω_x = mean streamwise vorticity, $[\partial(W/U_{C\ell})/\partial Y - \partial(V/U_{C\ell})/\partial Z]$

Subscript

$C\ell$ = centerline value

Introduction

THE turbulent square jet behaves like its round counterpart in the far flowfield. However, significant differences have been found[1] in the near-region behavior of these two symmetrical jet geometries The difference in the near-region behavior can be traced back to the evolution of the vortical structures that are formed as a result of the instabilities in these jets. Indeed, as is well known,[2] the curvature variation of a vortical structure in the azimuthal direction results in the nonuniform self-induction and hence the deformation of the vortical structure. Unlike a round vortical structure that has constant azimuthal curvature and will, therefore, not deform, a square vortical structure will, as a result of azimuthal curvature variation, be expected to deform. Abramovich[3] has hypothesized that a rectangular vortex ring will deform as a result of pressure imbalance between the long and short sides of the ring, the pressure on the long sides, which are closer to the major axis of the vortex ring, being lower than the pressure on the short sides, which are farther away from the vortex ring minor axis. According to the hypothesis of Abramovich, a square vortex ring should, therefore, not deform. The results of the present study show that the hypothesis of Abramovich, although plausible for rectangular jets, is inapplicable to square jets. It is recognized that the vortex rings may also deform as a result of mutual induction and/or interaction.

In the work of Quinn and Militzer,[1] the experimental and numerical results for the mean flow and turbulence quantities were reported only for the center plane and not the entire jet cross section. Although these results made it possible to show that the square jet spreads significantly faster than the round jet in the near region and that both jets spread at the same rate in the far flowfield, the deformation of the square jet cross section in the near region could not be shown by them. The only other study[4] devoted entirely to the square jet also reports only center-plane experimental and numerical results for the mean streamwise velocity and the spanwise Reynolds primary shear stress. Results for the decay of the mean streamwise velocity along the centerline of a turbulent free square jet have been reported in the rectangular jet studies of Trentacoste and Sforza[5] and McGuirk and Rodi.[6] Tsuchiya et al.[7] report, within the framework of an experimental study of rectangular jets, results for the jet half-velocity width growth of a square jet.

A study that examines the streamwise development of a turbulent square jet cross section is currently not available. Such a study is needed to illuminate the near-region deformation of a square jet cross section. The present study, which documents the results of detailed measurements of the mean streamwise velocity, the three Reynolds normal stresses, and the two Reynolds primary shear stresses, was done to satisfy such a need. Air was used as the jet fluid. The exit plane area of the square slot was 0.00161 m^2, and this resulted in an equivalent diameter, defined as the diameter of a round slot with same exit plane area as the square slot, of 0.0453 m. The exit plane Reynolds number, based on the equivalent diameter, was about 2.08×10^5. The mean streamwise velocity and streamwise turbulence intensity at the center of the slot exit plane were maintained at 60 m/s and 0.5%, respectively.

Experimental Details

A blow-down flow facility was used in the present study. This flow facility has been described elsewhere[1] in detail. Briefly, the flow facility, a sketch of which is shown in Fig. 1, consists of a centrifugal fan; a settling chamber fitted with a baffle, honeycomb, and mesh-wire screens; a three-dimensional contraction with a contour based on a third-degree polynomial; and the sharp-edged square slot. The slot is at-

Received Jan. 14, 1992; presented as Paper 92-02-045 at the DGLR/AIAA 14th Aeroacoustics Conference, Aachen, Germany, May 11-15, 1992; revision received May 12, 1992; accepted for publication May 18, 1992.

*Associate Professor, Department of Engineering. Member AIAA.

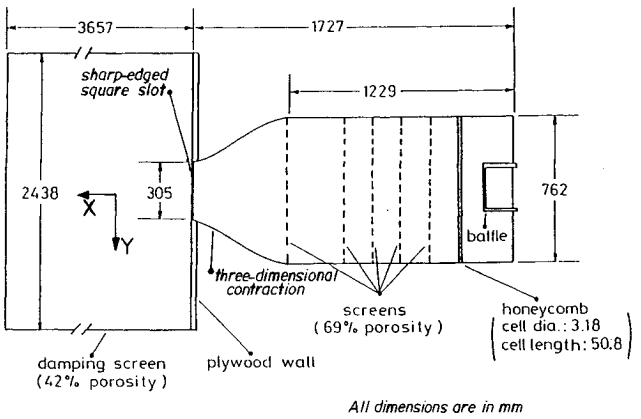

Fig. 1 Sketch of the flow facility.

tached to the downstream end of the three-dimensional contraction. The jet issues from the slot into a cage covered, on its top and sides, with steel damping screens of 42% porosity. The downstream end of the cage, which extends 3.66 m, is open, and the upstream end is fitted with a 2.44 × 2.44 m plywood wall that is flush with the exit plane of the three-dimensional contraction.

A three-dimensional traversing system, driven by stepping motors under microcomputer control, was used for moving the sensing probe in the flowfield. The traversing system employs a rack and pinion in the streamwise direction and lead screws in the spanwise and lateral directions. Figure 1 also shows a definition sketch of the coordinate system. The Z coordinate, which is perpendicular to the plane in which X and Y lie and forms a right-hand system with them, is not shown in Fig. 1. The sensing probe could be positioned to within 0.3 mm in the streamwise direction and to within 0.01 mm in the spanwise and lateral directions.

DANTEC P61 X-array hot-wire probes (made from platinum-coated tungsten wires 5 μm in diameter and 1.2 mm in active length), operated at a resistance ratio of 1.8 by DANTEC constant temperature anemometers, were calibrated on the jet centerline in the very near region against the output of a pitot-static tube. The pitot-static tube was connected to a pressure transducer and a Barocel electronic manometer. The calibration data were fitted to the hot-wire power law, and the three calibration constants were optimized by means of a linear least-squares goodness-of-fit procedure. A "cosine law" response to yaw was assumed, and the effective angle was determined from a yaw calibration as described by Bradshaw.[8] Temperature variations from the calibration temperature were monitored with a thermocouple placed close to the X-array hot-wire probe and corrections for such variations were made, following Bearman,[9] in the data reduction soft-

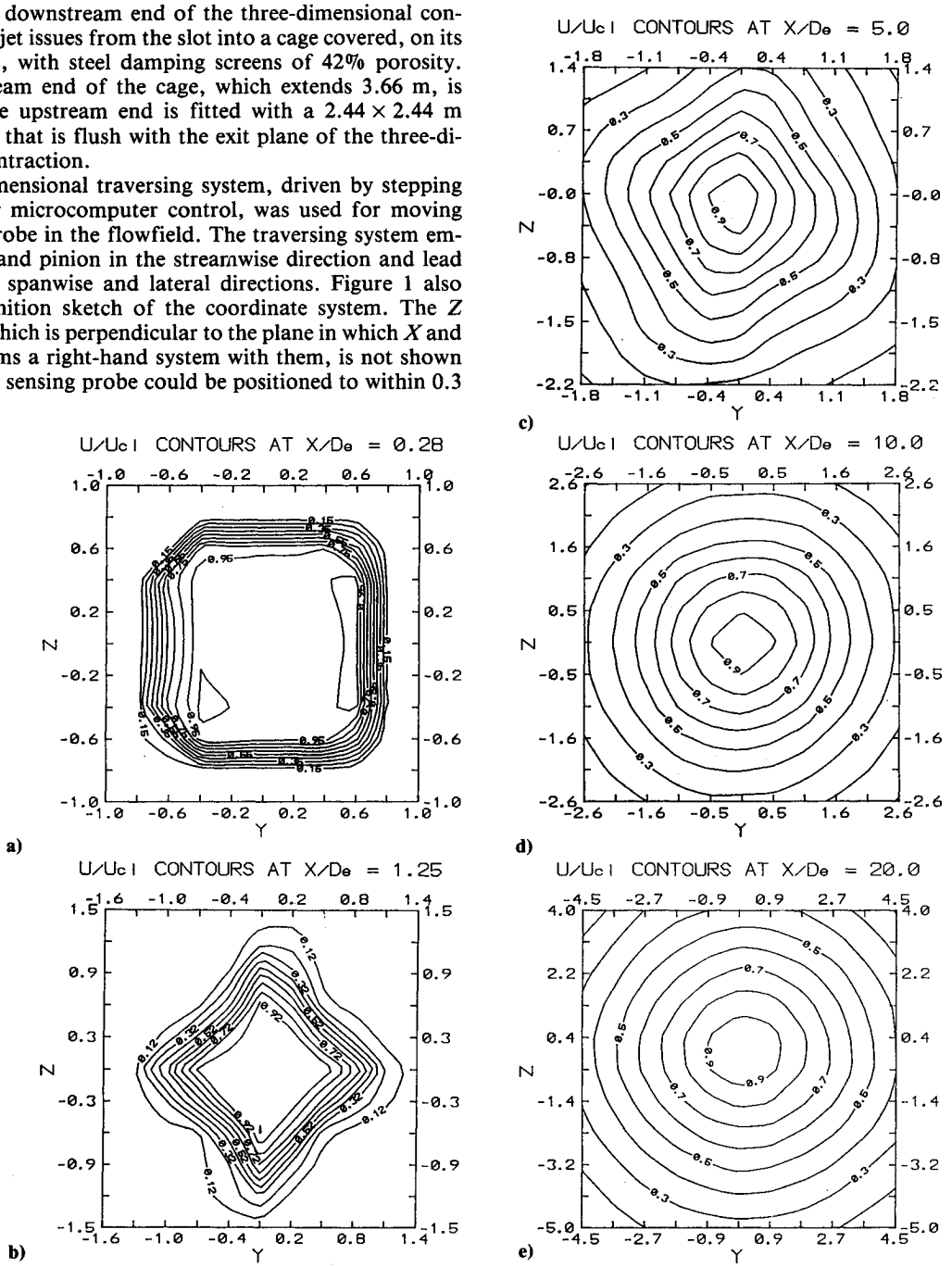

Fig. 2 Mean streamwise velocity contour maps.

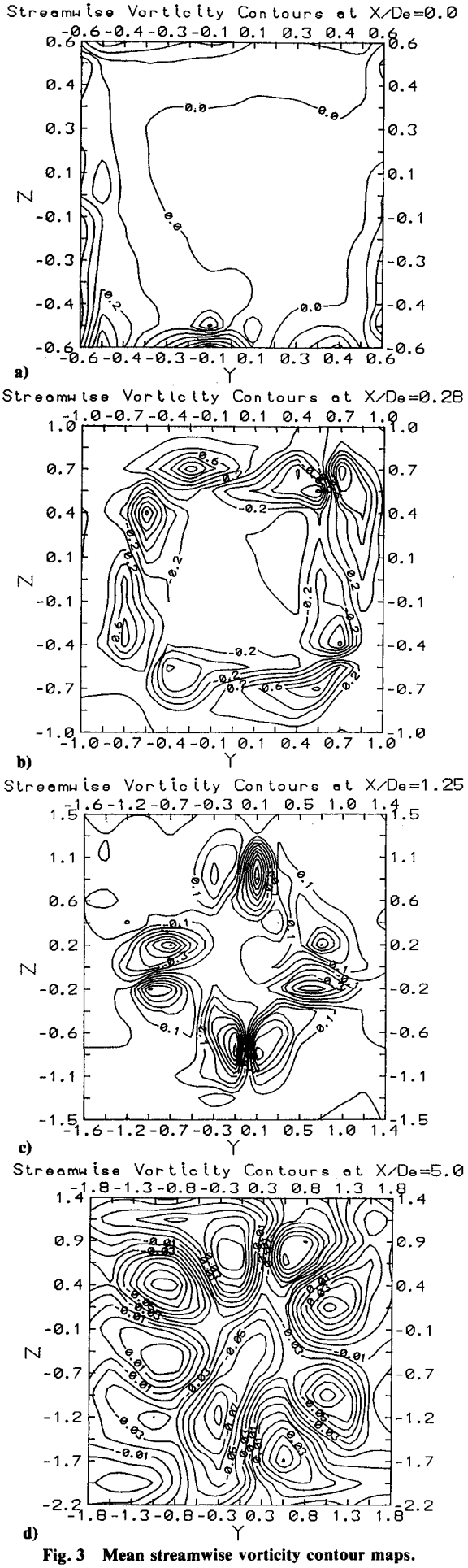

Fig. 3 Mean streamwise vorticity contour maps.

ware. The effect of tangential cooling of the X-array hot-wire sensors was accounted for by incorporating the correction formulas of Champagne and Sleicher[10] in the data reduction software. The analog signals from the X-array hot-wire probes were linearized by the laboratory microcomputer and digitized, at about 1 kHz, by a 12-bit successive approximation analog-to-digital (A/D) converter. As is well known,[11] samples of turbulent flow signals should, for statistical independence, be spaced approximately two integral time scales apart. The integral time scale for the present flow was estimated, from the size of the square slot (0.04 m) and the speed (60 m/s) of the flow at the slot exit plane, to be 6.67×10^{-4} s. The reciprocal of twice the integral time scale then results in a sampling rate of 750 Hz; the 1 kHz sampling rate is thus adequate. It is important to note that the sample size, which was an input variable in the data acquisition software, was selected such that the probe had a sufficient dwell time at each measurement location. Moreover, spectra and quantities involving derivatives were not measured. Two low-pass analog filters with

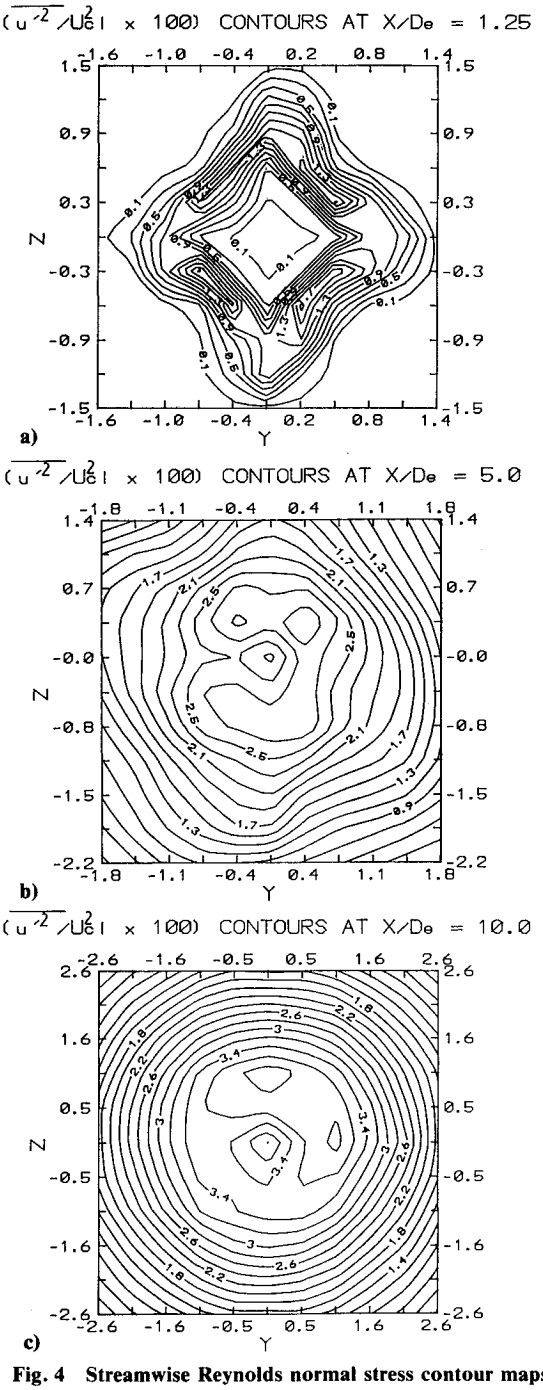

Fig. 4 Streamwise Reynolds normal stress contour maps.

amplifiers were used for signal conditioning. A two-channel sample-and-hold unit with very low droop rate was employed in the signal processing since the analog-to-digital conversion was done sequentially. The data reduction, to obtain the mean and fluctuating velocities, was done in real time.

Results and Discussion

Mean streamwise velocity contour maps at five streamwise locations are shown in Fig. 2. The data, from which the contour maps were obtained, were acquired on a grid at each streamwise measurement station. The grid spacing, which was kept constant at a given measurement station, was varied from 2.54 mm at $X/D_e = 0.28$ to 6.35 mm at $X/D_e = 10$ and beyond. The contour-plotting software employed a cubic spline for interpolation between data points. Close to the slot exit plane, at $X/D_e = 0.28$, the contours are very closely spaced, and they have the square shape prescribed by the slot. The very close spacing between the contour levels implies steep mean streamwise velocity gradients and very little entrainment of ambient fluid. The off-center mean streamwise velocity peaks, noted by Quinn and Militzer,[1] are also found in the present flow at $X/D_e = 0.28$. It should be noted that such off-center mean streamwise velocity peaks are an attribute of the existence of a vena contracta that is triggered by the sharp-edged exit of the slot. Farther downstream, at $X/D_e = 1.25$, the contours have acquired a "diamond" shape and the spacing between the contour levels has increased somewhat; the deformation of the jet cross section is clearly evident. At $X/D_e = 5.0$, the "diamond" shape is still present, and the contour levels are wider spaced, indicating more significant entrainment of ambient fluid. The mean streamwise velocity contours are fully axisymmetric at $X/D_e = 20$ and beyond. The estimated uncertainty in the measurement of the mean streamwise velocity is ± 1% at 20:1 odds. Note that the uncertainties, given subsequently, in the other measured quan-

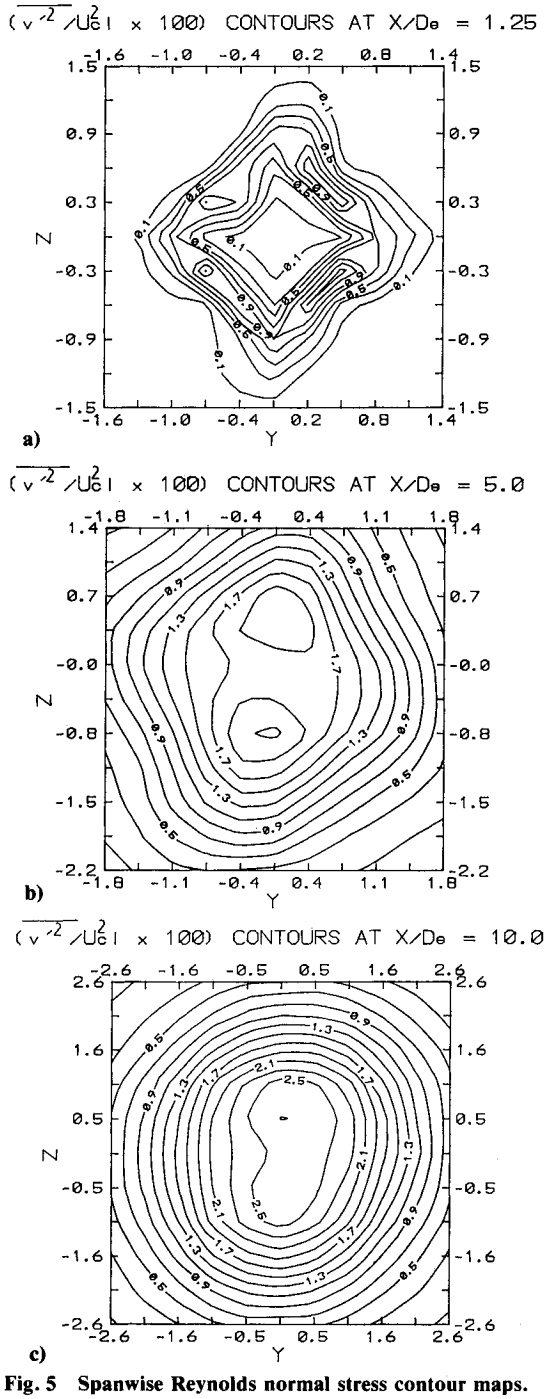

Fig. 5 Spanwise Reynolds normal stress contour maps.

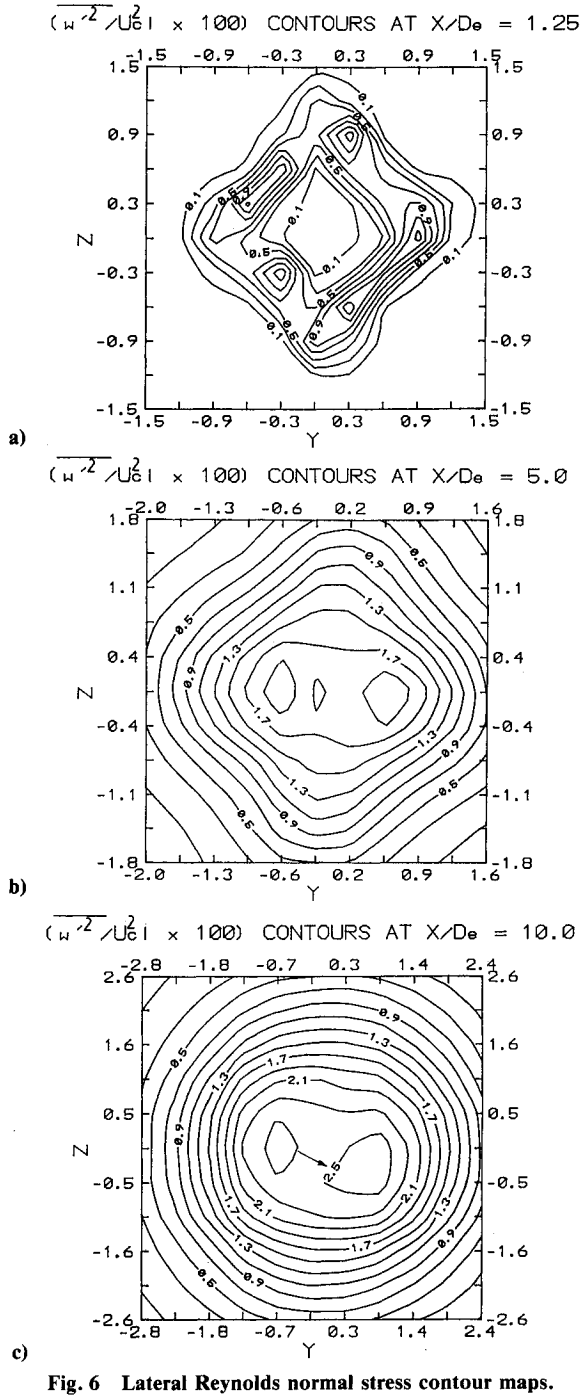

Fig. 6 Lateral Reynolds normal stress contour maps.

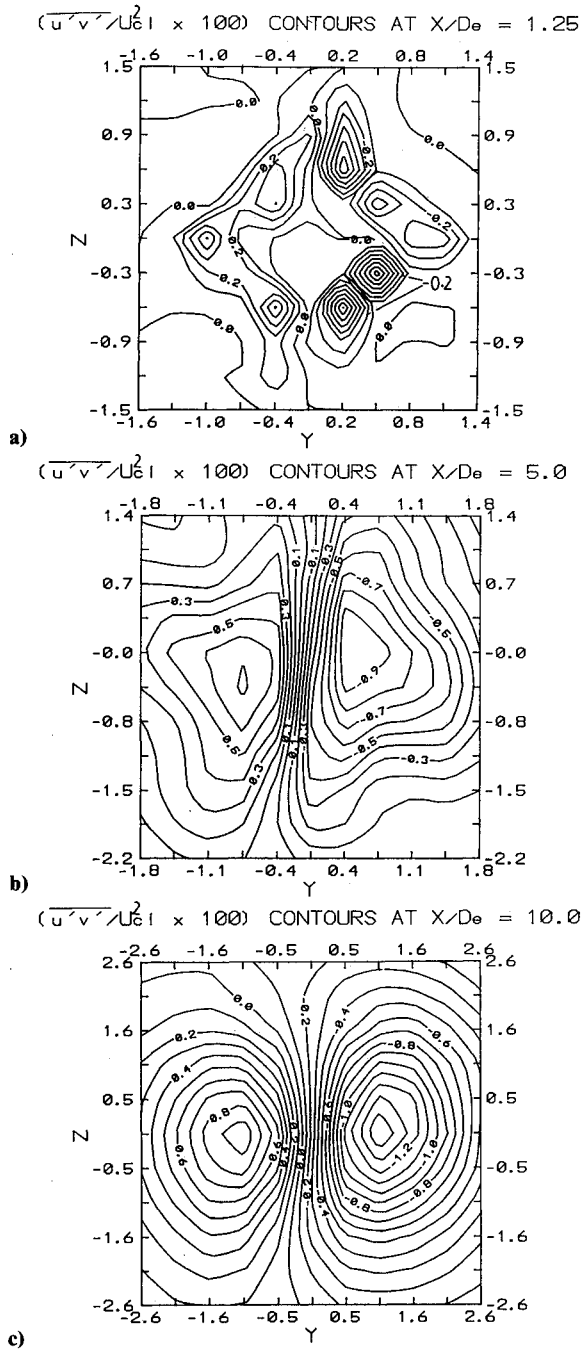

Fig. 7 Spanwise Reynolds primary shear stress contour maps.

tities will be at the same odds (i.e., 20: 1) and therefore will not be restated.

The mean streamwise vorticity was calculated from the mean spanwise velocity and mean lateral velocity data, and the results are shown as contour maps in Fig. 3. Note that positive and negative Ω_x indicate counterclockwise and clockwise rotation, respectively, in the present context. Discrete streamwise vortices are clearly identifiable at $X/D_e = 0.28$. These vortices, which represent Prandtl's secondary flow of the first kind, are generated from the distributed vorticity shed from the four corners of the slot by skewing of the shear layers as a result of the vena contracta effect. The vortices occur necessarily in counter-rotating pairs because they are generated within the body of a homogeneous fluid.[2] The vortex pairs move toward the center of the jet, as can be seen at $X/D_e = 1.25$ and 5.0, by mutual induction and are diffused by the turbulent stresses and viscosity. The vortex pairs also undergo deformation (i.e., stretching and tilting) by the action of various mean strain rates. It is indeed interesting to note the similarity between the deformation of the mean streamwise velocity field and that of the vortex pairs at $X/D_e = 1.25$ and 5.0. The uncertainty in the mean streamwise vorticity data is estimated to be $\pm 19.5\%$.

The streamwise, spanwise, and lateral Reynolds normal stress contour maps are shown in Figs. 4, 5, and 6, respectively. The shapes of the streamwise Reynolds normal stress contours are similar to those of the mean streamwise velocity contours shown in Fig. 3 at the corresponding streamwise locations. Large or small values of the streamwise Reynolds normal stress are found, as is to be expected,[8] at locations in the flowfield where large or small values of the local shear in the mean streamwise velocity occur. The spanwise and lateral Reynolds normal stresses, although approximately equal to each other, are generally smaller than the streamwise Reynolds normal stress; this should be expected since the spanwise and lateral fluctuating velocities acquire their energy, via the pressure fluctuations, from the streamwise fluctuating velocities.

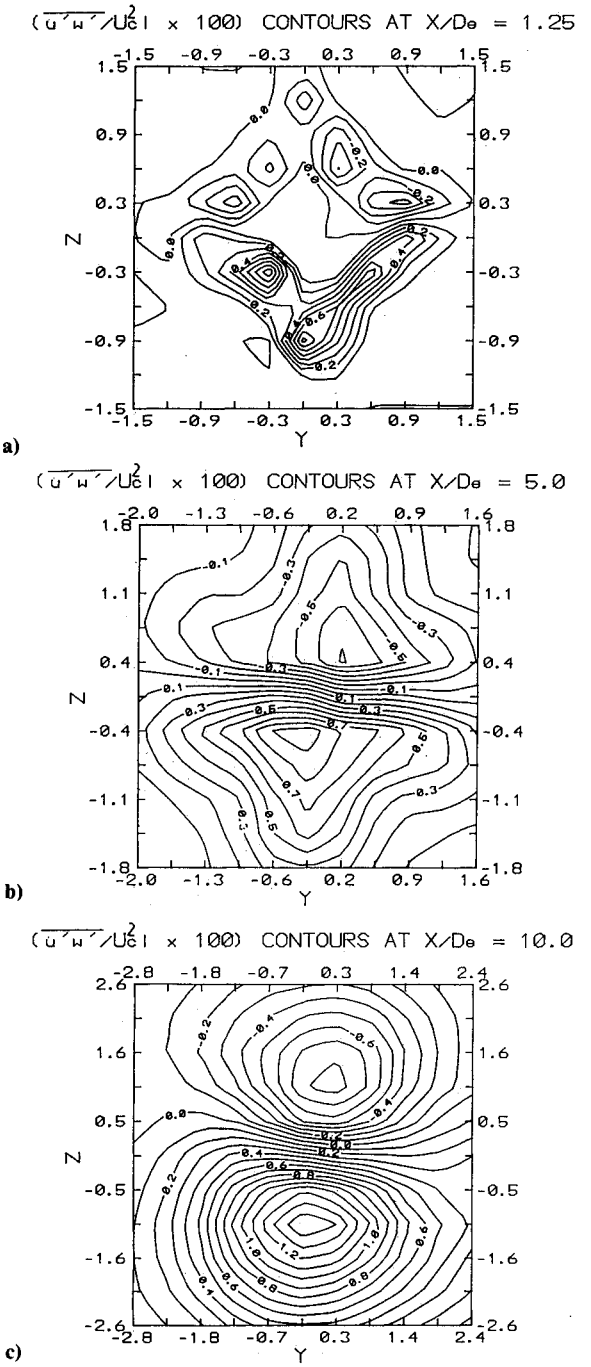

Fig. 8 Lateral Reynolds primary shear stress contour maps.

The maximum values of $\overline{u'^2}/U_{C\ell}^2 \times 100$, $\overline{v'^2}/U_{C\ell}^2 \times 100$, and $\overline{w'^2}/U_{C\ell}^2 \times 100$ at $X/D_e = 10$ in the present square jet study are 3.6, 2.5, and 2.5, respectively. The corresponding maximum values of these quantities at the same location in a round jet, from the study of Boguslawski and Popiel,[12] are 0.567, 0.146, and 0.125, respectively. The higher values of these turbulence quantities in the square jet provide evidence of faster mixing of the square jet compared with the round jet. The estimated uncertainty in the measurement of the Reynolds normal stresses is $\pm 6\%$.

The spanwise and lateral Reynolds primary shear stress contour maps are shown in Figs. 7 and 8, respectively. As is the case with the streamwise Reynolds normal stress, large values of the Reynolds primary shear stresses occur in flow regions where the local shear in the mean streamwise velocity is large. The maximum value of the Reynolds primary shear stress, $\overline{u'v'}/U_{C\ell}^2 \times 100$ at $X/D_e = 10$ in the present square jet is 1.4, which is higher than the value, 0.88,[12] in a round jet at $X/D = 12$; this provides further evidence of the known[1] faster mixing of the square jet. The estimated uncertainty in the measurement of the Reynolds primary shear stresses is $\pm 8\%$.

Tabulated numerical values of all of the data presented in this study can be obtained from the author upon request.

Conclusions

The present study of a turbulent free jet of air issuing from a sharp-edged square slot into still air surroundings has provided detailed time-averaged data for the mean streamwise velocity, mean streamwise vorticity, Reynolds normal stresses, and Reynolds primary shear stresses.

It was found that the near-region behavior of the jet is dominated by four sets of counter-rotating streamwise vortices. These vortices, which represent Prandtl's secondary flow of the first kind, are generated from distributed vorticity shed from the four corners of the slot by skewing of the shear layers as a result of the vena contracta effect. Mean streamwise velocity off-center peaks were also found in the very near region; such mean streamwise velocity off-center peaks may be the result of the self-induction of the streamwise vortices. Furthermore, the higher numerical values of the Reynolds normal and primary shear stresses in the present square jet, compared with those found in a round jet, indicate faster mixing of the square jet.

Acknowledgment

The support of the Natural Sciences and Engineering Research Council of Canada (NSERC) is gratefully acknowledged.

References

[1]Quinn, W. R., and Militzer, J., "Experimental and Numerical Study of a Turbulent Free Square Jet," *Physics of Fluids,* Vol. 31, No. 5, 1988, pp. 1017–1025.

[2]Batchelor, G. K., *An Introduction to Fluid Dynamics,* Cambridge Univ. Press, Cambridge, England, UK, 1967.

[3]Abramovich, G. N., "On the Deformation of the Rectangular Turbulent Jet Cross-Section," *International Journal of Heat and Mass Transfer,* Vol. 25, No. 12, 1982, pp. 1885–1894.

[4]duPlessis, M. P., Wang, R. L., and Kahawita, R., "Investigation of the Near-Region of a Square Jet," *Journal of Fluids Engineering,* Vol. 96, 1974, pp. 246–251.

[5]Trentacoste, N., and Sforza, P. M., "Further Experimental Results for Three-Dimensional Free Jets," *AIAA Journal,* Vol. 5, No. 5, 1967, pp. 885–891.

[6]McGuirk, J. J., and Rodi, W., "The Calculation of Three-Dimensional Turbulent Free Jets," *Proceedings of the 1st Symposium on Turbulent Shear Flows* (University Park, PA), April 1977, pp. 1.29–1.36.

[7]Tsuchiya, Y., Horikoshi, C., and Sato, T., "On the Spread of Rectangular Jets," *Experiments in Fluids,* Vol. 4, No. 4, 1986, pp. 197–204.

[8]Bradshaw, P., *An Introduction to Turbulence and Its Measurement,* Pergamon, Oxford, England, UK, 1974.

[9]Bearman, P. W., "Corrections for the Effect of Ambient Temperature Drift on Hot-Wire Measurements in Incompressible Flow," *DISA Information,* Vol. 11, May 1972, pp. 25–30.

[10]Champagne, F. H., and Sleicher, C. A., "Turbulence Measurements with Inclined Hot-Wire Probes—Part 2: Hot-Wire Response Equations," *Journal of Fluid Mechanics,* Vol. 23, Pt. 1, 1967, pp. 177–182.

[11]Larsen, P. S., and Buchhave, P., "Flow Measurements: Why, What and How? Part 2," *DANTEC Information,* Vol. 2, Jan. 1986, pp. 2–7.

[12]Boguslawski, L., and Popiel, C. O., "Flow Structure of the Free Round Turbulent Jet in the Initial Region," *Journal of Fluid Mechanics,* Vol. 90, 1979, pp. 531–539.